IEEE P802.11
Wireless LANs

Performance of the Proposed 5-GHz PHY

Date: Month Day, Year

Author: John H. Cafarella
MICRILOR, Inc.
17 Lakeside Office Park, Wakefield, MA 01880
Phone: 617-246-0103
Fax: 617:246-0157
e-Mail: JohnCafarella@worldnet.att.net

Abstract

This is a first draft documenting the performance of the 5-GHz proposal. It is currently incomplete, especially in the area of multipath & noise performance. It is to be re-issued in approximately one month.

1 Performance Summary

1.1 Implementation

RF/IF nothing special relative to other implementations

Baseband chip ≈ 25K gates modem function + 10K gates control

Diversity not considered, but no major impact on circuitry.

1.2 Immunity or Multipath and Noise

Multipath analysis still in progress.

1.3 Overhead Related Parameters

PLCP Preamble & Header < 30 μs (diversity not included)

Slot size 25 μs; similar to 802-11.15

SIFS could be short, depending upon processor.

1.4 Spectral Efficiency and Cell Density Related Parameters

Channelization: Six 24-Mbps frequency channels

Eight search code channels

48 cyclic data code channels
64K pseudorandom code channels

Cell Planning: BSAs operated with substantial spatial overlap of user areas if on different frequency channels; BSAs on same frequency channel is reasonable separation; always separate code channels as a matter of practice.

Adjacent channel interference: On same frequency channel, desired signal must exceed interfering signal by ≈ 8 dB. For different frequency channels there is extra 35 dB isolation (as in low-rate standard); could be 40-45 dB with margin.

Interference Immunity

>14-dB processing gain against CW
12-dB processing gain against >25% BW Gaussian noise

1.5 Critical Points

- Phase noise not an issue
- Power consumption attractive
- Complexity not an issue
- RF PA backoff 6 dB; not required for 18 Mbps mode
- Antenna diversity separable issue

1.6 Intellectual Property

Letter to IEEE in preparation. Patents pending. Will comply with IEEE guidelines. Policy by 1 March; call Dr. Stanley Reible.

2 Multipath Models

2.1 Infinitely Diffuse Rayleigh (IDR)

The Infinitely Diffuse Rayleigh path model assumes that the channel impulse response comprises Rayleigh-distributed paths at discrete, uniformly spaced delays, filled in delay

$$h_c(t) = \sum_{k=0}^{\infty} a_k \delta(t - k\tau_s)$$

where τ_s is the delay spacing, and a_k is a complex amplitude whose real and imaginary components are Gaussian-distributed, with the following equivalent distributions:

$$p(\mathrm{Re}\{a_k\}) = \frac{1}{\sqrt{2\pi}\sigma_k} e^{-\frac{\mathrm{Re}\{a_k\}^2}{2\sigma_k^2}}$$

$$p(\mathrm{Im}\{a_k\}) = \frac{1}{\sqrt{2\pi}\sigma_k} e^{-\frac{\mathrm{Im}\{a_k\}^2}{2\sigma_k^2}}$$

real/imaginary components

$$p(|a_k|) = \frac{|a_k|}{\sigma_k^2} e^{-\frac{|a_k|^2}{2\sigma_k^2}}$$

$$p(Arg\{a_k\}) = \frac{1}{2\pi}$$

magnitude & phase

The path strengths are exponentially distributed in amplitude vs. delay

$$\sigma_k^2 = \frac{1 - e^{-\frac{\tau_s}{T_s}}}{2} e^{-\frac{k\tau_s}{T_s}}$$

where T_{RMS} is the multipath RMS delay spread. The normalization of the path strengths holds the total received signal power constant as other parameters are varied. The multipath-delay spacing is the shorter of the spread-spectrum chip time T_c or half the delay spread T_{RMS}.

3 Signal Model

The transmit waveform[1] has the baseband representation

$$s(t) = \sum_n j^n c_n p_{MSK}(t - nT_c)$$

where

T_c is the inverse of the chip frequency,
n is the chip index within a symbol,
there are M=16 chips per symbol,
m is the symbol index,
C_{mn} is the chip code, and
$p_T(t)$ is the single-chip waveform:

During the acquisition preamble the chip value is

$$c_n = C_{S,n \bmod M}$$

where

C_{Sn} is the search PN code, 0≤n<M-1.

In the data portion of a frame the chip value is

$$c_n = d_{n \bmod M} C_{n \bmod M, n} W_{K_m n}$$

where

d_{ms} is the polarity specified by the DBPSK component of the 4-ary DBOK signaling in sub-channel s,
P_{mn} is the PN code during the m^{th} symbol,
W_{Kmsn} is the sub-channel s Walsh function during the m^{th} symbol, and
K_{ms} is specified by the 4-ary OK signaling component in sub-channel s.

When transmitted, s(t) is convolved with the channel impulse response to yield the received waveform

$$r(t) = \sum_{k=0}^{\infty} a_k \sum_n j^n c_n p_{MSK}(t - kt_s - nT_c)$$

At the receiver complex Gaussian noise z(t) is added, which obeys

$$\overline{z(t)} = 0$$

$$\overline{z(t) z(t')} = 0$$

$$\overline{z(t)^* z(t')} = 2N_0$$

where N_0 is the one-sided noise spectral density. The waveform is then convolved with the aggregate receive filter to form x(t)=w(t)+q(t). The deterministic part w(t) (i.e., r(t) filtered) is

$$r(t) = \sum_{k=0}^{\infty} a_k \sum_n j^n c_n p_{MSK}(t - kt_s - nT_c)$$

where $p_R(t)$ is the chip-pulse waveform after receive filtering.
The noise component q(t) (i.e., z(t) filtered) has variance

[1] See Appendix on MSK Approximation.

$$\overline{|q(t)|^2} = \overline{\frac{1}{T_c}\int z^*(\sigma)\cos(\frac{\pi(t-\sigma)}{2T_c})d\sigma \ \frac{1}{T_c}\int z(\sigma')\cos(\frac{\pi(t-\sigma')}{2T_c})d\sigma}$$
$$= \frac{2N_0}{T_c^2}\int \cos^2(\frac{\pi(t-\sigma)}{2T_c})d\sigma = \frac{2N_0}{T_c^2}$$

where B_N is the noise bandwidth of the receiver.

The filtered receive waveform is sampled at the chip rate to produce the sequence $x_n=w_n+q_n$.

$$r(t) = \sum_{k=0}^{\infty} a_k \sum_n j^n c_n p_{MSK}(t - k\tau_s - nT_c)$$

The statistics of samples of the noise q_n will be the same as q(t). During acquisition the strongest path (at some delay $k_0\tau_s$) is selected for demodulation. We explicitly define the sampling time reference to correspond to the correct sampling time for the first chip of symbol m_0 on this strongest signal component; that is, we select $t_0=k_0\tau_s+m_0MT_c$. Thus, the signal sequence is

$$r(t) = \sum_{k=0}^{\infty} a_k \sum_n j^n c_n p_{MSK}(t - k\tau_s - nT_c)$$

The correlator reference sample sequence is $j^{-n}B_{m0n}$;[2] the correlator output is

$$r(t) = \sum_{k=0}^{\infty} a_k \sum_n j^n c_n p_{MSK}(t - k\tau_s - nT_c)$$

A number of chip values can contribute to the n^{th} sample because of the width of $p_R(t)$ and also because of the multipath delay spread. It is most natural to measure the delay spread in multiples, or sub-multiples, of the chip time because it simplifies analysis and simulations. For 0 delay spread we have a Gaussian channel; when the delay spread is a single chip time, then it is necessary to half-chip sampling of the multipath profile; for integer multiples greater than 1 the multipath profile is sampled at the chip time. The multipath will thus be sampled at T_c or $\frac{1}{2}T_c$; the possible sampled values of $p_R(t)$ are[3]

$$\overline{|q(t)|^2} = \overline{\frac{1}{T_c}\int z^*(\sigma)\cos(\frac{\pi(t-\sigma)}{2T_c})d\sigma \ \frac{1}{T_c}\int z(\sigma')\cos(\frac{\pi(t-\sigma')}{2T_c})d\sigma}$$
$$= \frac{2N_0}{T_c^2}\int \cos^2(\frac{\pi(t-\sigma)}{2T_c})d\sigma = \frac{2N_0}{T_c^2}$$

Samples at $1.5T_c$ or greater from the time of the peak are approximately zero. We can make the replacement

$$r(t) = \sum_{k=0}^{\infty} a_k \sum_n j^n c_n p_{MSK}(t - k\tau_s - nT_c)$$

where the function[4] $\delta_x=1$ if the index equals 0, and $\delta_x=0$ otherwise).

[2] Although the correlator reference will be properly aligned to the signal, it is necessary to provide for mismatch of the reference and signal to later support 16-ary Orthogonal demodulation.

[3] Because of the linearity of filtering, the chip pulse is approximately symmetric.

[4] This is the Kronecker delta δ_{x0} with half-integer values of x allowed.

$$r(t) = \sum_{k=0}^{\infty} a_k \sum_{n} j^n c_n p_{MSK}(t - kt_s - nT_c)$$

Observations:

- The first term is the principal contribution for each path, i.e., samples at the peak of the chip waveform.

- The second two terms (having coefficients $p_{R½}$) are introduced when the multipath is sampled at half the chip time.

- The last two terms (coefficients p_{R1}) reflect the inter-chip effects of using, MSK or filtered PSK.

This may be further developed by specializing to multipath sampling at the chip time or half that value. In the following two equations, the expression in braces {} is a required constraint on remaining variables to be consistent with the original limits on the summation over n'. Note that in all cases this constraint has the form {0 ≤ n+Δ ≤ M-1}.

For $\tau_s=T_c$

$$r(t) = \sum_{k=0}^{\infty} a_k \sum_n j^n c_n p_{MSK}(t - kt_s - nT_c)$$

For $\tau_s=\frac{1}{2}T_c$

$$r(t) = \sum_{k=0}^{\infty} a_k \sum_n j^n c_n p_{MSK}(t - kt_s - nT_c)$$

We introduce the acyclic correlation function $R_{BC\Delta}$ as follows:

$$r(t) = \sum_{k=0}^{\infty} a_k \sum_n j^n c_n p_{MSK}(t - kt_s - nT_c)$$

This is a standard definition of the crosscorrelation of code sequences, except that the $j^{-\Delta}$ factor introduced by MSK signaling has also been absorbed into the definition.[5] With this, the above equations become

[5] This is convenient analytically, and it also means that the results can be used directly for PSK waveforms as well as for MSK.

For $\tau_s=T_c$

$$r(t) = \sum_{k=0}^{\infty} a_k \sum_n j^n c_n p_{MSK}(t - kt_s - nT_c)$$

For $\tau_s=½T_c$

$$r(t) = \sum_{k=0}^{\infty} a_k \sum_n j^n c_n p_{MSK}(t - kt_s - nT_c)$$

These equations represent the outputs Y of correlators matched to reference codes B, due to input codes C at various multipath delays. It is necessary to further specialize these to consider signal demodulation and detection performance; this will be done in the next two sections.

The receiver filtering will be intentionally broadened relative to ideal matched filtering to avoid excessive inter-chip ISI (keep p_{R1} small); thus, the noise will be uncorrelated from sample to sample. The noise variances of correlator outputs is

$$\overline{|q(t)|^2} = \overline{\frac{1}{T_c}\int z^*(s)\cos(\frac{p(t-s)}{2T_c})ds \ \frac{1}{T_c}\int z(s')\cos(\frac{p(t-s')}{2T_c})ds}$$
$$= \frac{2N_0}{T_c^2}\int \cos^2(\frac{p(t-s)}{2T_c})ds = \frac{2N_0}{T_c^2}$$

When multiple correlator outputs are considered, the correlator noise is uncorrelated between correlators because the reference functions are orthogonal.

In the following sections, we shall focus on delay spreads greater than or equal to $2T_c$. This avoids considerable analytical complexity, since sampling at $\tau_s=T_c$ avoids handling correlations induced by sampling the multipath at half the chip rate. This restricts our attention to delay spreads ≥62.5 ns for the 32-Mchip/s modulation.

4 Demodulation Performance

4.1 Demodulation Mode Formulation

We begin with the expression for the correlator outputs specialized to the case of 4x4-ary signaling, where the transmitted waveforms are $c_n = d_{n \bmod M} C_{n \bmod M, n} W_{K_m n}$ and the correlators are matched to $B_m = P_m W_K$. The correlator outputs for symbol m_0 are

$$r(t) = \sum_{k=0}^{\infty} a_k \sum_n j^n c_n p_{MSK}(t - kt_s - nT_c)$$

From here on we shall neglect the terms in p_{R1}. These reflect inter-chip effects due to bandwidth reduction, for example as encountered when PSK signals are filtered, and in any case for MSK-like signals. The value of p_{R1} is approximately .2; by contrast we must consider correlation side lobes of order .5 or higher relative to the autocorrelation peak, and multipath amplitudes which can be equal to the path being demodulated. Thus, the effects reflected by carrying the p_{R1} terms are of second-order in significance, and carrying them would complicate the analysis without benefit. The correlator outputs are

$$r(t) = \sum_{k=0}^{\infty} a_k \sum_n j^n c_n p_{MSK}(t - kt_s - nT_c)$$

We expect that symbol waveform m_0 can be significantly effected by the two immediately preceding symbols and the following symbol, for any multipath model. For 2 Msymbol/s signaling this is a span of 2 μs. Over this range of symbols we expand the sum

$$r(t) = \sum_{k=0}^{\infty} a_k \sum_n j^n c_n p_{MSK}(t - kt_s - nT_c)$$

In addition to the above signal components there is thermal noise. The correlator outputs are Rician-distributed with SNR

$$r(t) = \sum_{k=0}^{\infty} a_k \sum_n j^n c_n p_{MSK}(t - kt_s - nT_c)$$

The probability of symbol error, conditioned on the specific waveforms $\mathbf{s} = \left\{ \sum_{\mathbf{s}=\mathbf{0}}^{\mathbf{3}} P_{m_0+1} W_{K_{m_0+1}, s}, \sum_{s=0}^{3} P_{m_0} W_{K_{m_0} s}, \sum_{s=0}^{3} P_{m_0-1} W_{K_{m_0-1}, s}, \sum_{s=0}^{3} P_{m_0-2} W_{K_{m_0-2},} \right\}$ and the multipath profile $\mathbf{a} = \{a_0, a_0, a_0 \ldots\}$, is

$$P_e\big|_{\mathbf{s},\mathbf{a}} = 1 - \prod_S \int_0^\infty dr_{K_{m_0 s}} \frac{r_{K_{m_0 s}}}{\sigma^2} e^{-\frac{r_{K_{m_0 s}}^2}{2\sigma^2} - \gamma_{K_{m_0 s}}} I_0\left(\frac{r_{K_{m_0 s}}}{\sigma^2}\sqrt{2\gamma_{K_{m_0 s}}}\right) \prod_{K \neq K_{m_0 s}} \left[\int_0^{r_{K_{m_0}}} dr_{K_s} \frac{r_{K_s}}{\sigma^2} e^{-\frac{r_{K_s}^2}{2\sigma^2} - \gamma_{K_s}} I_0\left(\frac{r_{K_s}}{\sigma^2}\sqrt{2\gamma_K}\right) \right]$$

In general it is necessary to average this probability of error over relevant distributions for **s** and **a**.

4.2 Gaussian channel

For the Gaussian channel we have $|\alpha_0|^2=1$ and (hence $k_0=0$) and $\alpha_k=0$ ($k>0$), so the signal component of the detection correlator outputs[6] are

$$r(t) = \sum_{k=0}^{\infty} a_k \sum_n j^n c_n p_{MSK}(t - kT_s - nT_c)$$

where δ_{nm} is the conventional Kronecker delta. These are the outputs of 16 correlators matched to the waveform set generated by combining the PN code used for the m^{th} symbol P_{m0} with each of the 16 Walsh functions W_J. The output[7] SNR is

$$r(t) = \sum_{k=0}^{\infty} a_k \sum_n j^n c_n p_{MSK}(t - kT_s - nT_c)$$

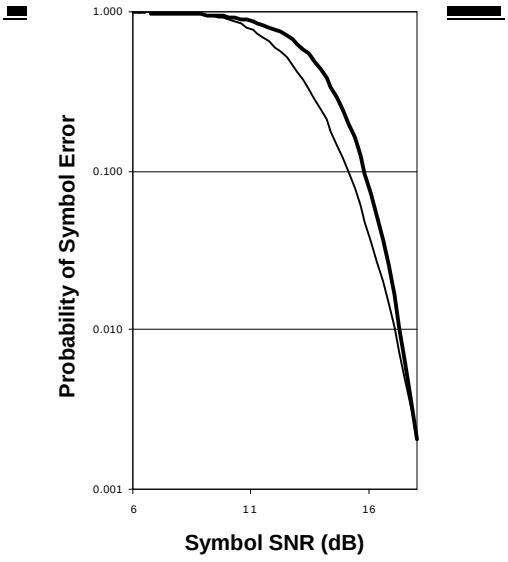

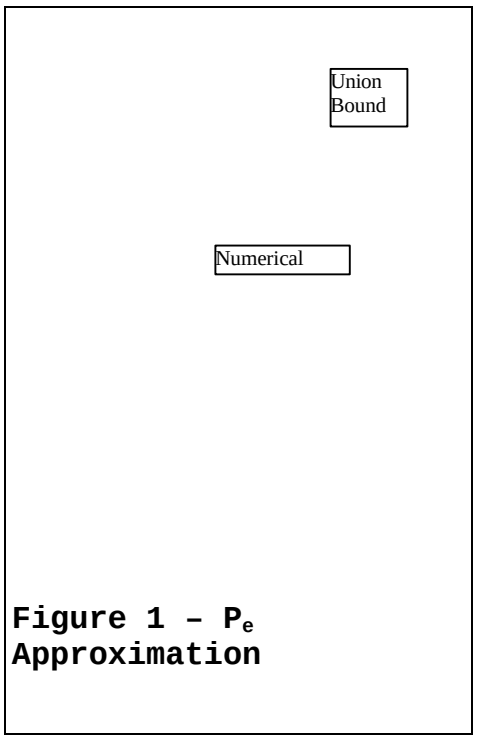

Figure 1 – P_e Approximation

We may evaluate the error probability for 4x4-ary OK[8] using the union bound

[6] α_0 still carries an unknown propagation phase.
[7] If a true matched filter were used, then this would be the familiar E/N_0.

$$P_e(\gamma) \approx 1-(1-\tfrac{3}{2}e^{-\frac{\gamma}{2}})^4$$

The exact OK probability of error is given by

$$P_e = 1-\left[\int_0^{\infty} dr_1 \frac{r_1}{\sigma^2} e^{-\frac{r_1^2}{2\sigma^2}-\gamma} I_0\left(\frac{r_1}{\sigma^2}\sqrt{2\gamma}\right)\left[\int_0^{r_1} dr_2 \frac{r_2}{\sigma^2} e^{-\frac{r_2^2}{2\sigma^2}}\right]^3\right]^4$$

where r_1 is the Rician variate of the correct correlator output in a sub-group of four, and r_2 represents the Rayleigh variates of the other three incorrect correlator outputs. This has no closed-form solution, which is, of course, why the approximation is needed. Figure 1 compares numerical evaluation of the integrals to the approximation.

4.3 IDR Channel, $T_{RMS} \ddagger 2T_c$

THIS SECTION IN PROGRESS

[8] We shall evaluate the probability of symbol error based only upon the orthogonal-signaling component; in the absence of such errors, the error probability for the DBPSK component is completely negligible.

5 Detection Performance

5.1 Acquisition Mode Formulation

The signal model was formulated to support analysis of Noncoherent BiOrthogonal Keying with PN codes changing from symbol to symbol. In this section we specialize to the acquisition signal; i.e., a 16-chip code C_{Sn} repeated from symbol to symbol. The codes and their cyclic correlations are tabulated in section Appendix: **Search Codes**. The cyclic correlation of two codes[9] is

$$r(t) = \sum_{k=0}^{\infty} a_k \sum_n j^n c_n p_{MSK}(t - k\tau_s - nT_c)$$

Consider the primary contribution (peak of chip waveform) to a correlator output Y_B for symbol m_0 due to a unit-amplitude signal component at delay $k\tau_s$

$$r(t) = \sum_{k=0}^{\infty} a_k \sum_n j^n c_n p_{MSK}(t - k\tau_s - nT_c)$$

where we have recognized that the two acyclic correlations in each case actually make up the full cyclic correlation (using $j^M=1$). The correlator output, with the reference matched to and aligned with the signal at lag k_0T_c, is

$$r(t) = \sum_{k=0}^{\infty} a_k \sum_n j^n c_n p_{MSK}(t - k\tau_s - nT_c)$$

During the search phase, the signal is repeated continually; the cyclic correlation function, in effect, aliases multipath components delayed by one or multiple symbols, whereas during demodulation these become intersymbol interference. We now explore this fold-over effect.

There are only MT_c possible sample times within the periodic symbol timing (assuming delay spread $\geq 2T_c$). Multipath at lag $(mM+n)T_c$ appears summed with multipath at lag nT_c, for all m. Because of this, we may re-cast the multipath description by summing multipath components separated by multiples of MT_c. For path models having strengths which are complex Gaussian, such a summation will also be complex Gaussian (Rayleigh amplitude). For example, the re-cast (cyclic) IDR channel impulse response is

$$h_c(t) = \sum_{k=0}^{\infty} a_k \delta(t - k\tau_s)$$

where[10]

$$\sigma_k^2 = \frac{1 - e^{-\frac{\tau_s}{T_s}}}{2} e^{-\frac{k\tau_s}{T_s}}$$

[9] We use ~ (tilde) to distinguish cyclic correlations from acyclic.

[10] Note that the normalization is preserved, i.e., summing $\sigma^2_{\beta k}$ over the corresponding range of k.

5.2 Gaussian channel

For the Gaussian channel we have $|\alpha_0|^2=1$ and (hence $k_0=0$) and $\alpha_k=0$ ($k>0$), so the signal component of the detection correlator output[11] is

$$r(t) = \sum_{k=0}^{\infty} a_k \sum_n j^n c_n p_{MSK}(t - kt_s - nT_c)$$

and the output[12] SNR is

$$r(t) = \sum_{k=0}^{\infty} a_k \sum_n j^n c_n p_{MSK}(t - kt_s - nT_c)$$

The probability of detection vs. γ for a given probability of false alarm may be found as the non-fluctuating-target case in books on radar, e.g., DiFranco and Rubin,[13] although the reader is cautioned that radar texts generally use $R=2\gamma$ as the signal to noise, whereas communication texts use γ.

5.3 IDR Channel, $T_{RMS} \ddagger 2T_c$

Although the search correlator employs the same single-sample-per-chip computation as does the demodulation correlator, this is actually stepped along at half-chip intervals to limit the "straddling loss" to a fraction of a dB. During demodulation k_0 corresponds to the strongest multipath; during acquisition k_0 can be considered a hypothesis to be tested, i.e., whether the signal at delay $k_0\tau_s$ exceeds the threshold. Thus, we may compute the probability of detection as one minus the probability that correlator outputs for $k_0=0$ to M-1 all fall below the threshold. The correlator outputs for the k_0 are

$$r(t) = \sum_{k=0}^{\infty} a_k \sum_n j^n c_n p_{MSK}(t - kt_s - nT_c)$$

We ignore autocorrelation side lobes, assuming

$$r(t) = \sum_{k=0}^{\infty} a_k \sum_n j^n c_n p_{MSK}(t - kt_s - nT_c)$$

which results in

$$r(t) = \sum_{k=0}^{\infty} a_k \sum_n j^n c_n p_{MSK}(t - kt_s - nT_c)$$

To the same level of approximation, we can set $p_{R1}=0$ for detection since it is lower than expected autocorrelation side lobes. For a single-component Rayleigh-fluctuating signal the probability of detection vs. mean signal-to-noise ratio and probability of false alarm is given by[14]

$$P_d = P_{fa}^{1/(1+\bar{\gamma})}$$

Where γ is the mean SNR. For detection we test correlator amplitudes for M times of arrival, and the signal is missed only if detection fails on all M. For signal timing corresponding to k_0, the mean path SNR for the IDR channel is

---

[11] α_0 still carries an unknown propagation phase.
[12] If a true matched filter were used, then this would be the familiar E/N_0.
[13] DiFranco and Rubin, Radar Detection.
[14] Op Cit, DiFranco and Rubin.

$$r(t) = \sum_{k=0}^{\infty} a_k \sum_n j^n c_n p_{MSK}(t - kt_s - nT_c)$$

The definition of $\overline{SNR}_{TOT}$ comes from

$$s_k^2 = \frac{1 - e^{-\frac{t_s}{T_s}}}{2} e^{-\frac{kt_s}{T_s}}$$

independent of T_{RMS} for the IDR channel. Thus, the probability of detection in multipath is

$$P_d = 1 - \prod_{k_0=0}^{M-1} \left(1 - P_{fa}^{1/(1+M\, 2s_{bk_0}^2\, \overline{SNR})}\right)$$

5.4 Performance

Figure 2 shows the probability of missed detection vs. mean input SNR for the IDR channel, and vs. SNR for the Gaussian channel, for a detection criterion requiring threshold crossings on three successive symbols, at overall probability of false alarm of 10^{-6}. Requiring multiple threshold crossings enables improvement of detection performance, relative to single-symbol detection, without incurring the complexity of video combining before testing against a threshold. If we budget 1% of frame loss to missed detection, then it is clear from the figure that IDR multipath spreads from about 60 to 250 ns will incur 4- to 5-dB of fading loss, but that detectability improves monotonically with SNR.

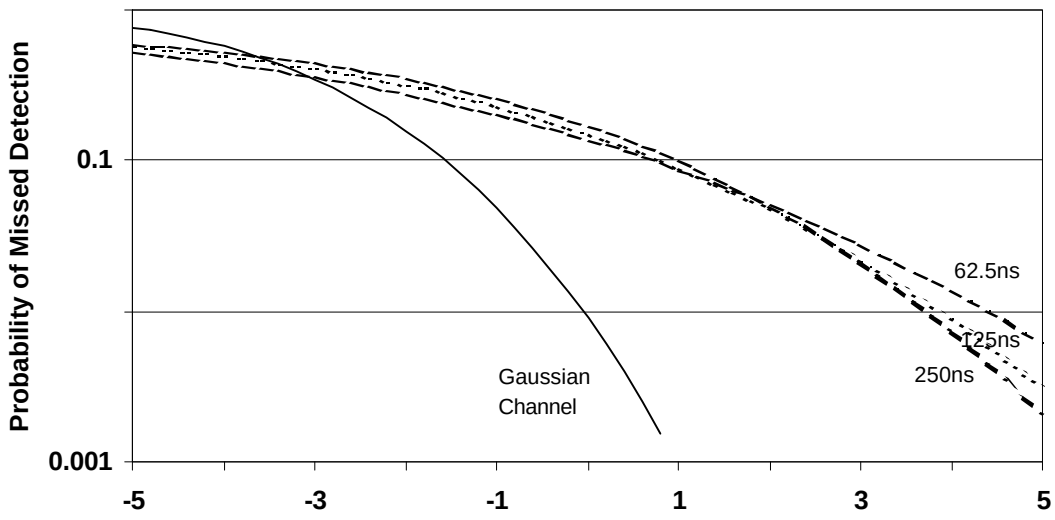

Figure 2 - Detection Performance

6 Interference Rejection

Previous sections assessed link performance in noise and multipath. This section considers interference rejection in the absence of multipath propagation effects.

6.1 Interference Rejection Formulation

From Gaussian **channel** the signal response for the mth symbol is[15]

$$r(\ ) = \sum_{=0}^{\infty} a_k \sum_n j \quad {}_n p_{MSK}\ t \qquad - nT_c)$$

where P_m is the PN code, J represents the Walsh-function correlator outputs and K_{ms} are the signal variants transmitted, respectively, ${}_0$ is the signal strength and ${}_{nm}$ is the Kronecker delta.

$x(t)e^{j2\pi\nu t}$, where x(t) is the envelope and ν is the offset frequency. It is assumed that the bandwidth of x(t) is small enough, and that ν is restricted to be sufficiently close to the signal carrier frequency, that no substantial roll-off due to receive filtering can be included in the processing gain calculation. The interference is sampled and applied to the correlator bank to produce

$$r(t) = \sum_{k=0}^{\infty} a_k \sum_n j^n c_n p_{MSK}(t - k\mathrm{t}_{\ s} - nT_c)$$

We consider next the cases of narrowband CW interference and of band-limited Gaussian interference.

6.2 Narrowband CW Interference

We assume the interference to be $I\,e^{j2\pi\nu t}$, where I is the complex amplitude of the interference. The correlator outputs are

$$r(t) = \sum_{k=0}^{\infty} a_k \sum_n j^n c_n p_{MSK}(t - k\mathrm{t}_{\ s} - nT_c)$$

As shown in document IEEE P802.11-97/116, for CW interference there is an abrupt drop to zero probability of error for some CW interference level when the largest possible interference output can no longer influence the data decision. We may determine this threshold by finding

[15] We have ignored here the p_{R1} terms as second-order.

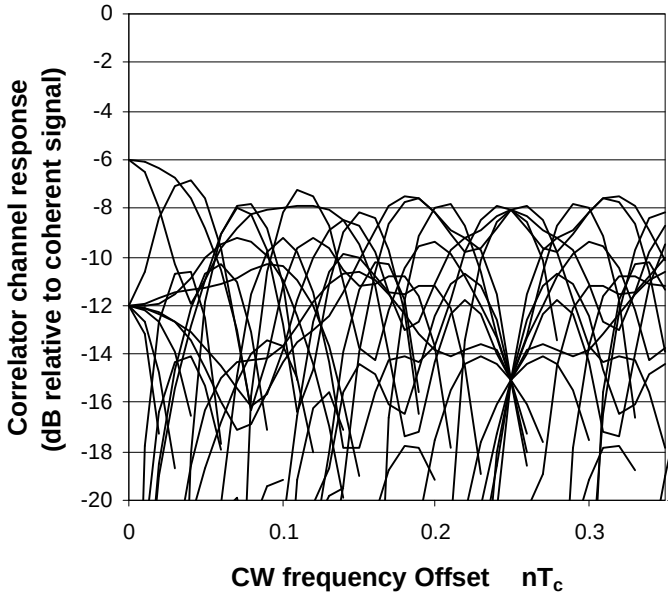

Figure 3 - Correlator output responses.

$$r(t) = \sum_{k=0}^{\infty} a_k \sum_n j^n c_n p_{MSK}(t - kt_s - nT_c)$$

for the (M=16 bit) PN codes to be used. The 8 PN codes (coset leaders) have identical statistics in this regard. We show here the case of $P_{mn}=0158_H$. Figure 1 shows $r(t) = \sum_{=0}^{\infty} a_k \sum j\ c\ p \quad (t \quad kt \quad nT)$ (measured in dB relative to coherent response) vs. νT_c for all 16 correlator outputs. The worst-case situation occurs for ν within a symbol bandwidth of center frequency, where 2 correlator outputs produce outputs only 6-dB down from a coherent signal. As the CW interference level approaches the zero-error threshold, it is only the two channels having –6-dB responses for the interference which are of interest. With approximately ¼ probability both of these channels fall in the same sub-set of Walsh functions. The signal would emerge from one of these two channels, and it is possible for the CW interference to produce an amplitude out of an incorrect channel while simultaneously lowering the amplitude of the correct channel. An error will occur when

$$\left|\frac{I}{2} \quad a_0\right| \le \left|\frac{}{2}\right|$$

Taking the arbitrary phase angle between the interference and signal to be Θ, an error occurs for

$$\left|\frac{2I}{0} \quad 1\right| \le \left|\frac{2I}{a}\right| \quad \text{or} \quad 1 + 4\left|\frac{I}{a_0}\right|^2 \quad 2\left|\frac{I}{}\right|\cos(\Theta) \le 4\left|\frac{I}{a_0}\right|^2$$

Θ_B

making an error and angles for which no error occurs. The solution for this angle is

$$\cos(\Theta_B) = -\left|\frac{2I}{a_0}\right|^{-1} = -\sqrt{g/4} \quad \textbf{where } g \equiv \frac{|a_0|^2}{|I|^2}$$

is the signal-to-interference ratio. There clearly can be no error for $\gamma>4$; for $\gamma<4$ the solution for Θ_B is

$$\Theta_B = \pm\cos^{-1}(-\sqrt{g/4})$$

The random phase Θ is distributed over 2π, so the probability of error is simply the fraction of 2π for which an error will occur times the ≈1/4 probability that the correct channel is one of the two channels under consideration, or

$$P_e(\gamma) = \frac{1}{4\pi}\cos^{-1}(\sqrt{\gamma/4})$$

It must be remembered that this is the asymptotic behavior near γ=4; for low signal-to-interference ratio the probability of error is larger than indicated by the above expression.

6.3 Narrowband Gaussian Interference

In this case we assume that x(t) is a Gaussian random variable. The correlator outputs due to noise are

$$r(t) = \sum_{k=0}^{\infty} a_k \sum_n j^n c_n p_{MSK}(t - kT_s - nT_c)$$

It is assumed that the noise bandwidth is small enough, and that the frequency offset is confined, such that no substantial roll-off due to receive filtering is included as processing gain.

The processed interference remains Gaussian, since the correlation process is linear, so it remains only to find the mean-square correlator outputs.

$$r(t) = \sum_{k=0}^{\infty} a_k \sum_n j^n c_n p_{MSK}(t - kT_s - nT_c)$$

In the case of white Gaussian noise, the correlator outputs are equal-variance, uncorrelated Gaussian variables. The above equation can be used to explore the effect of the bandwidth of the Gaussian interference. $P_m=0158_H$ was used, combined with the 16 Walsh functions to calculate the correlator outputs shown in Figure 4.

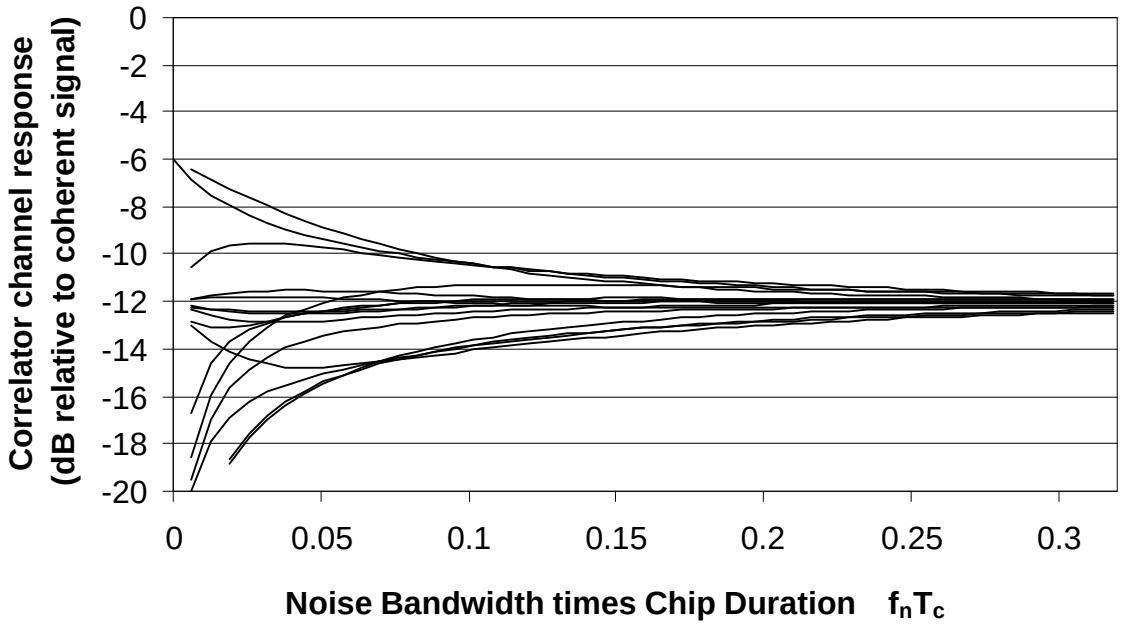

Figure 4 - Correlator output varainces, normalized to $2\sigma^2$, in dB relative to coherent response.

For very narrowband Gaussian interference ($a \rightarrow 0$) anomalous results are obtained. Two of the correlator outputs produce interference outputs suppressed only 6 dB relative to the coherent signal; this is due to lack of one-zero balance in the code for those correlator channels. On the other hand, six of the correlator outputs provide essentially infinite rejection of narrowband interference. The remaining eight outputs yield the same 12-dB suppression of narrowband interference as is the case for wideband interference.

Asymptotically ($a \rightarrow \infty$) all 16 correlator outputs produce the 12-dB suppression of the Gaussian interference expected from the 16 chips per symbol. It is clear that for noise bandwidths greater than approximately 25% of the chip rate (or 4 times the symbol rate) the processing gain is essentially the nominal 12 dB.

As shown above, 4x4-ary OK splits the signal between the four sub-set channels, incurring 6-dB reduction of signal amplitude.

6.4 Performance

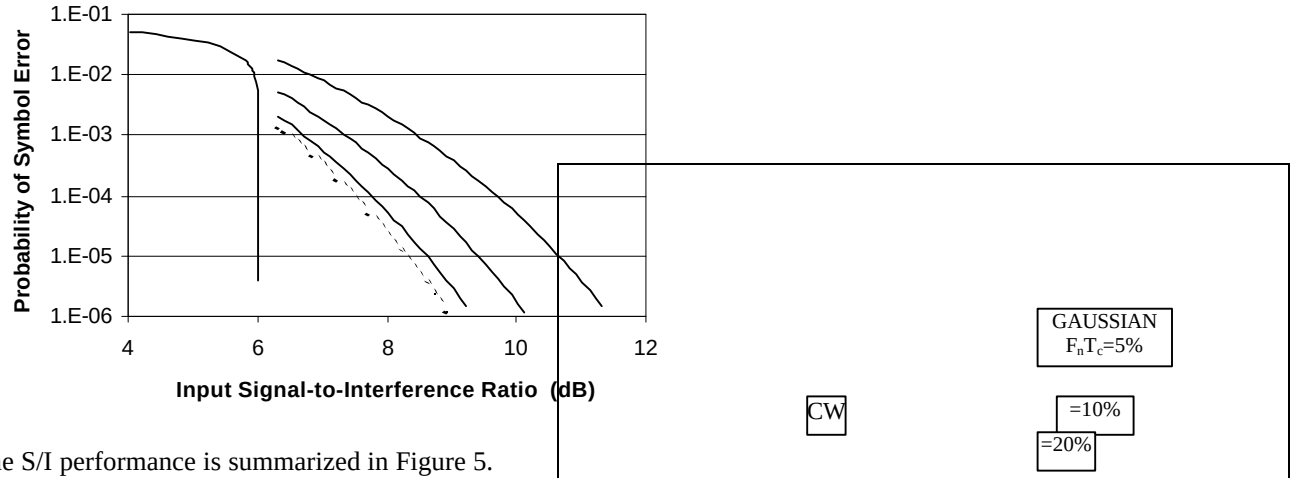

Figure 5 – Symbol error probability for CW and Gaussian interference

The S/I performance is summarized in Figure 5. CW interference produces a large error probability until the S/I approaches 0 dB, at which point the probability of error drops abruptly to zero. For Gaussian interference the probability of error was estimated using the union bound, with the signal emerging from the correlator channel having the smallest variance; that is, summing the binary-orthogonal error probabilities for S/I set by the (largest) individual channel responses to the interference. This was done for 5%, 10% and 20% noise bandwidth relative to the chip rate (f_nT_c). Also shown is the asymptotic behavior if the noise were decorrelated from chip to chip[16]. At 20% noise bandwidth the performance is within a fraction of a dB of the asymptotic behavior for large noise bandwidth.

Interpreting this curve in terms of the "processing gain" test,[17] the dashed curve (decorrelated-noise limit) represents the 12-dB which is ten times $\log_{10}$ of the number of chips per symbol; CW interference would appear to have PG of 14 dB, while Gaussian noise at 10% and 5% would yield 10.9-dB and 9.7-dB, respectively.

[16] This ignores the receive filtering reduction on the noise, but this limit is simply for comparison.
[17] The implementation loss is assumed the same for all cases.

7 Appendix: Approximate MSK

The 12-bit/symbol modulation exhibits a 6-dB peak/average amplitude fluctuation. The individual chip waveforms will have the shape of MSK chip pulses, although their amplitudes will fluctuate. The result will be an average power spectrum which appears the same as for MSK. In the 9- and 5-bit/symbol modes the waveforms are truly of constant envelope, hence these will be MSK transmissions in fact. The approximation to MSK to be implemented departs from an ideal, matched MSK system in the following:

a) the generation process combines a staircase approximation to a cosine pulse followed by a filter to offer an inexpensive implementation;

b) the transmit spectrum has lower side bands than ideal MSK;

c) the receive processor does not exactly match the chip waveform, preferring to keep the bandwidth somewhat higher for better multipath resolution.

The ideal MSK waveform has the baseband representation

$$s(t) = \sum_n j^n c_n p_{MSK}(t - nT_c)$$

where

T_c is the inverse of the chip frequency,
n is the chip index,
c_n is the chip value, and
$p_{MSK}(t)$ is the single-chip MSK waveform:

$$p_{MSK}(t) = \cos(\frac{\pi t}{2T_c}) \quad |t| < T_c$$
$$= 0 \quad |t| < T_c$$

Ideal processing of the MSK waveform at the receiver begins with the (analog) chip matched filter[18] (CMF) for the MSK pulse.

$$p_{CMF}(t) = \frac{1}{T_c}\cos(\frac{\pi t}{2T_c}) \quad |t| < T_c$$
$$= 0 \quad |t| < T_c$$

which results in the baseband waveform

$$w(t) = \sum_{k=0}^{\infty} a_k \sum_n j^n c_n R_{MSK}(t - kt_s - nT_c)$$

where the chip autocorrelation function is

$$R_{MSK}(t) = (1 - \frac{|t|}{2T_c})\cos(\frac{\pi t}{2T_c}) + \frac{1}{\pi}\sin(\frac{\pi t}{2T_c}) \quad |t| < 2T_c$$
$$= 0 \quad |t| > T_c$$

By contrast, the proposed implementation begins with a generator for the chip waveform which produces

[18] The filter's lack of causality is of no concern for present purposes.

$$p_{CMF}(t) = \frac{1}{T_c}\cos(\frac{\pi t}{2T_c}) \quad |t| < T_c$$
$$= 0 \qquad\qquad |t| < T_c$$

The transmit filtering is designed to minimize the energy taken out of the main spectral lobe while suppressing the side lobes. This may be accomplished using, e.g., 5th–order baseband filters plus some IF bandpass filter. As a result of this filtering, the generated pulse shape is replaced by the transmitter (equivalent-baseband) pulse shape $p_T(t)$, where

$$s(t) = \sum_n j^n c_n p_{MSK}(t - nT_c)$$

so that the baseband representation of the transmitter waveform is

$$s(t) = \sum_n j^n c_n p_{MSK}(t - nT_c)$$

On receive, the waveform is passed through equivalent IF and baseband filtering. The resulting baseband complex signal is

$$s(t) = \sum_n j^n c_n p_{MSK}(t - nT_c)$$

where $p_R(t)$ is

$$s(t) = \sum_n j^n c_n p_{MSK}(t - nT_c)$$

Of significance is that the pulse shape of $P_R(t)$ is of considerably less time extent that would be the case for a true MSK pulse passed through an exact chip matched filter. Chip-to-chip amplitude overlap with this approach is typically less than .2, compared to .5 for true MSK. This is important for good multipath performance.

8 Appendix: Search Codes

The 16-bit codes selected for use during search and C_{Sn} are given in the following table, along with their cyclic autocorrelation functions, symmetric about the main lobe.

C_{Sn} (hex)	R_{ss0}	R_{ss1}	R_{ss2}	R_{ss3}	R_{ss4}	R_{ss5}	R_{ss6}	R_{ss7}	R_{ss8}
44BC	16	0	0	0	0	0	-4	0	-4
A0DC	16	0	0	0	0	0	-4	0	-4
D223	16	0	0	0	0	0	-4	0	-4
0A76	16	0	0	0	0	0	-4	0	-4
425C	16	0	0	0	0	4	0	-4	0
23A4	16	0	0	0	0	4	0	-4	0
245C	16	0	0	0	0	-4	0	4	0
A243	16	0	0	0	0	-4	0	4	0

These codes have excellent correlation properties for signal detection and selection of the strongest multipath component, having 4 or 5 zero values for autocorrelation side lobes nearest to the main lobe. When it is required to select codes for independent operation of BSAs, it is important to consider the peak and average cross-correlation values between the different codes (dB relative to main lobe) as shown below.

	44BC		A0DC		D223		0A76	
	Peak	rms	peak	rms	Peak	rms	Peak	rms
44BC	0	-19.3	-2.5	-11.3	-6.0	-11.3	-6.0	-11.3
A0DC	-2.5	-11.3	0	-19.3	-6.0	-11.3	-6.0	-11.3
D223	-6.0	-11.3	-6.0	-11.3	0	-19.3	-2.5	-11.3
0A76	-6.0	-11.3	-6.0	-11.3	-2.5	-11.3	0	-19.3
425C	-4.1	-12.0	-8.5	-12.0	-4.1	-12.0	-4.1	-12.0
23A4	-4.1	-12.0	-4.1	-12.0	-4.1	-12.0	-8.5	-12.0
245C	-4.1	-12.0	-4.1	-12.0	-4.1	-12.0	-8.5	-12.0
A243	-4.1	-12.0	-8.5	-12.0	-4.1	-12.0	-4.1	-12.0

	425C		23A4		245C		A243	
	Peak	rms	peak	rms	Peak	rms	Peak	rms
44BC	-4.1	-12.0	-4.1	-12.0	-4.1	-12.0	-4.1	-12.0
A0DC	-8.5	-12.0	-4.1	-12.0	-4.1	-12.0	-8.5	-12.0
D223	-4.1	-12.0	-4.1	-12.0	-4.1	-12.0	-4.1	-12.0
0A76	-4.1	-12.0	-8.5	-12.0	-8.5	-12.0	-4.1	-12.0
425C	0	-18.1	-6.0	-11.1	-6.0	-13.3	-6.0	-13.3
23A4	-6.0	-11.1	0	-18.1	-6.0	-13.3	-6.0	-13.3
245C	-6.0	-13.3	-6.0	-13.3	0	-18.1	-6.0	-11.1
A243	-6.0	-13.3	-6.0	-13.3	-6.0	-11.1	0	-18.1